RSC Sustainability

ROYAL SOCIETY OF CHEMISTRY

TUTORIAL REVIEW

View Article Online
View Journal | View Issue

Cite this: *RSC Sustainability*, 2023, **1**, 1672

3D printing for flow biocatalysis

Elena Gkantzou,[a] Marie Weinhart[bc] and Selin Kara *[ad]

Received 17th May 2023
Accepted 8th August 2023

DOI: 10.1039/d3su00155e

rsc.li/rscsus

Additive manufacturing has evolved at such a level nowadays that it follows the sustainability pathways, from applied materials to processing costs. This is a fundamental reason that more and more scientific effort is devoted to incorporating this technology in different research fields. Implementation of 3D printing technology in flow biocatalysis can be addressed at every process design level, (i) either the reactor itself, (ii) the support material for biocatalyst confinement, or (iii) the peripheral accessories that can establish a highly controlled process. 3D printing is an attractive option for enabling the development of more efficient processes, along with facile performance optimization. Moreover, the 3D printing of a biocatalyst entrapped in a protecting scaffold offers an alternative immobilization approach with promising results for a cost-effective and green process design.

Sustainability spotlight

Flow systems have become part of numerous research laboratories in academia and industry, while biocatalytic systems have long been described as the sustainable alternative to classical chemical catalysis. Thus, there are increasing requirements for systems and devices that sustainably support biocatalytic flow systems. Additive manufacturing can be employed in different stages of a flow bioprocess, offering the scientists the benefit of customizing the equipment and even enhancing the system's productivity with tailor-made reactors and biocatalyst supports. The goals for sustainable consumption and production (UN-SDG12) can be addressed in this work, with literature examples of laboratory practices that promote functionality and longevity of industrially-relevant bioprocesses. An overview of recycling trends and time-to-process management is also described.

1. Introduction

Additive manufacturing (AM), or, as it is commonly known, three-dimensional (3D) printing, connects the virtual world with the objects we get in our hands in everyday life. The AM ecosystem consists of hardware, software/modeling, and materials; in its ideal form, it is a closed-loop system. This means that nowadays, 3D printing is focusing on sustainable sources of printing materials (inks, resins, and filaments) and follows pathways for recycling and chemical circularity.[1–3] The goal is to make AM a production technology whose products undergo the maximum possible reusing. At the end of their lifetime, every product either biodegrades or is recycled back into material feedstock.[4] If we add the low – or extremely low in some cases – processing costs of this technology, we can talk about a sustainability diamond, ready to be employed in a vast range of distinct technological sectors, from health and chemistry to mechanics, aerospace, and environmental applications.[5]

Additive manufacturing processes have also been implemented in the field of flow biocatalysis. This emerging application of biocatalysis is defined as the processes that take place under continuous flow conditions in specially designed reactor systems, elaborating biocatalysts either isolated, *i.e.*, enzymes, or in their whole-cell form.[6] The answer to why perform biocatalysis in flow reactors has been comprehensively answered by Tamborini *et al.* (2018)[7] and De Santis & Meyer *et al.* (2020)[8] in their reviews for biocatalytic process intensification. Prof. Polona Žnidaršič-Plazl has also reported on the promises and challenges of biotransformations in microflow.[9] In these and several other works,[10–12] it has been highlighted the substantial improvement in space-time yields (STYs) – a fundamental parameter used to describe the productivity in biocatalytic processes – when shifting from batch to continuous flow systems.[13–15] So, it can be argued that flow reactors are used when continuous productivity is of utmost importance, and there is no specific need for products at large scales. However, this is not entirely true. Scale-up of flow processes can be realized utilizing parallelization and numbering-up approaches. By doing so, production on a bigger scale can be more economically feasible if we consider the significantly smaller equipment, the decrease in reaction time from hours to minutes, and the highly controlled systems that can be realized when we have to do with small dimensions.[7] So, more efficient reactions and minimized waste production? industry's blessings.

[a]*Institute of Technical Chemistry, Leibniz University Hannover, 30167 Hannover, Germany. E-mail: selin.kara@iftc.uni-hannover.de*

[b]*Institute of Physical Chemistry and Electrochemistry, Leibniz Universität Hannover, 30167 Hannover, Germany*

[c]*Insitute of Chemistry and Biochemistry, Freie Universität Berlin, 14195 Berlin, Germany*

[d]*Biocatalysis and Bioprocessing Group, Department of Biological and Chemical Engineering, Aarhus University, 8000 Aarhus, Denmark. E-mail: selin.kara@bce.au.dk*

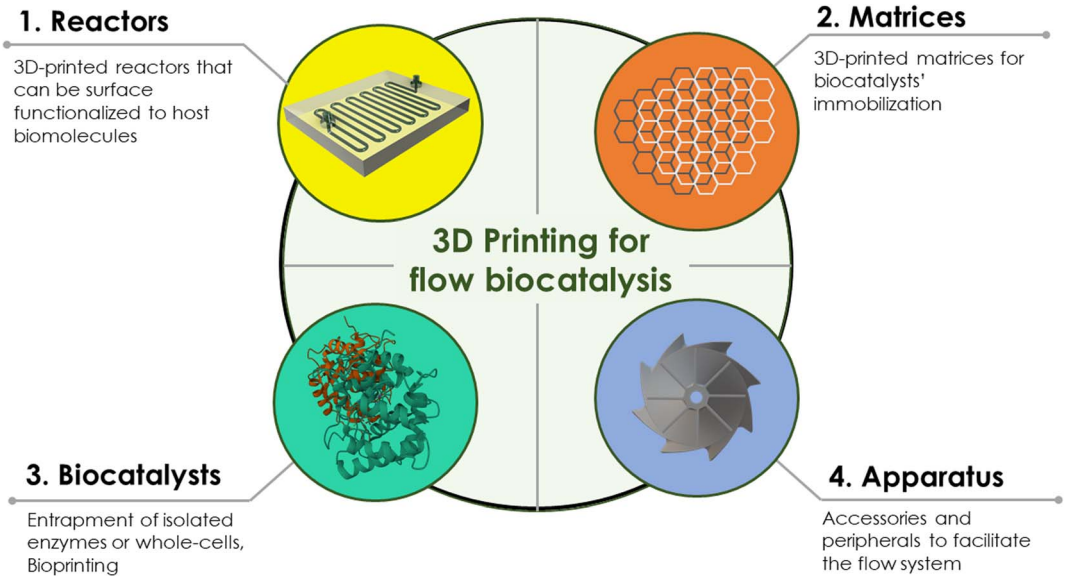

Fig. 1 The different ways to incorporate 3D printing in flow biocatalysis systems.

Nevertheless, how 3D printing technology is incorporated into flow systems design? For flow chemistry, we need reactors and/or peripherals like pumps, sensors, reservoirs, *etc.* For biocatalysis, a highly controlled microenvironment in a confined space is required, that can be translated to a chemically modified scaffold to host the biocatalyst, a defined reaction chamber with sufficient nutrients or substrates supply, or a specially designed reactor that could serve special needs like light penetration in photobiocatalysis.[16,17] 3D printing can do all of these. 3D-printed parts have been elaborated in all stages of a continuous flow biocatalytic process: (i) the reactor itself, (ii) the support material for biocatalyst confinement, or (iii) the peripheral accessories that can establish a highly controlled process.[18] Going with the 3D printing concept, rather than using already patented reactors, scaffolds, and accessories, offers the critical advantage of customizable products, fitted to the particular needs of each process. It can also be a relatively economical alternative since materials applied for 3D printers, or the 3D printers themselves, are becoming cheaper and more user-friendly. Complex geometries with high porosity can be realized, and a 'trial-and-error' method can be adopted by the user. Another critical aspect is that the software for 3D design is readily available to everyone, with multiple open-source programs, and a vast online community supporting the users in their endeavors.

In their review, Zentel *et al.* (2020) explored the potential of 3D printing for chemical reaction engineering.[19] They highlighted the impact of tailor-made designs and fabrication techniques as a game-changer in constructing reactors and downstreaming units in flow chemistry. Within this review article, we aim to bring together the reported knowledge in elaborating 3D printing for flow biocatalysis. We will delve into the scientific community's different approaches to utilize this flourishing technology to upgrade the continuous flow biocatalytic systems. Our approach is to divide the literature into 3D printing of reactors and reactor matrices (Section 2), 3D printing of biocatalysts (Section 3), and 3D printing of reactor apparatus (Section 4) necessary for the flow system performance (Fig. 1). This review aims to contribute to the existing literature for applying AM techniques in different fields of study. To the best of our knowledge, it is the first review with a special focus on flow biocatalysis.

2. 3D printing of reactors and reactor matrices for flow biocatalysis

In flow biocatalysis, biotransformations typically occur within confined spaces in reactors or reactor matrices, which both can be 3D-printed. At first, it was just an appropriate scaffold, chemically inert and mechanically stable. But nowadays, AM has evolved so that chemical functionalities can easily be added to initially inert printing materials. Matrix materials, blended materials, or reactive moieties have been explored in this context, offering superior performance to the 3D-printed scaffolds.[18,19] Recently, it was also reported a novel hydrogel as a reactor packing material produced with a mild 3D printing process.[20] One step further, the functionalities on the 3D-printed reactor surface can be used for targeted material–biosystem interactions, with enzyme immobilization being the most common approach.[21] Studies have shown that when the biocatalyst is fixed in the reactor surface, significant advantages in terms of stability and reusability arise.[22] So, the process follows the route: choose the appropriate material, 3D-print the scaffold, integrate the biocatalyst, and finally connect to the overall fluidic system.

Previous reports have reviewed the 3D printing techniques used for bio-related applications, including descriptions of the diverse materials that have been investigated.[18,19,21,23] In the following paragraphs, we will examine some relevant examples

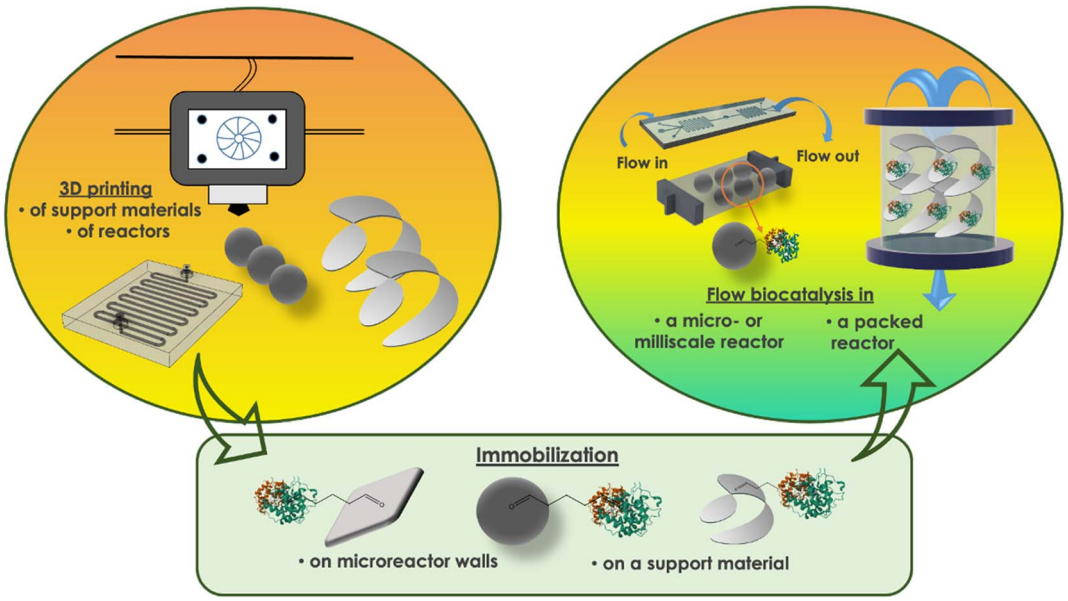

Fig. 2 3D printing of reactors and reactor matrices for flow biocatalysis.

from the literature, where 3D printing was elaborated for scaffold design and development in flow biocatalysis (Fig. 2). Table 1 summarizes the referenced literature.

2.1 3D printing the reactors

2.1.1 Milli-scale reactors. One of the first and simplest examples in this category was described by Peris *et al.* (2017), who were the first to establish a 3D-printed continuous flow reactor for ω-transaminase immobilization.[24] It was a milli-scale reactor developed by selective laser sintering (SLS) with a powder-based nylon material. This approach enabled the sequential chemical modification of the 3D-printed device with amino moieties to covalently bind the enzyme on the reactor surface. The optimization of the immobilization strategy was performed in a multi-well plate that was 3D-printed from the same material, showcasing the versatility of 3D printing for laboratory practices. After transferring the optimized protocols to the 3D-printed reactors, the continuous flow kinetic resolution of *rac*-methylbenzylamine was demonstrated. The system showed remarkable stability, maintaining its activity and selectivity with an enantiomeric excess (ee) over 94% after 78 hours of use, with a total of 105 catalytic cycles performed with the same immobilized enzyme. In the same concept of modification of the reactor surface using known chemicals, was the work of Ye *et al.* (2019).[25] This work investigated the performance of differently shaped scaffolds (diamond or honeycomb cubes, spheres, and pyramids) as carriers for enzymes from different classes. The best-performing sphere-shaped scaffolds were finally integrated into the reactor. The printing material used here was carbon fiber-reinforced polylactic acid (C-PLA). PLA filament is one of the most widely used fused deposition modeling (FDM) materials due to its low cost, easy handling, and recyclability. Carbon fibers were used as an additive for improved and adjustable chemical properties. The factors affecting the surface activation method for the scaffold were extensively studied by monitoring enzyme activity. The optimized protocol was applied for immobilizing different enzymes verified by producing valuable compounds like amoxicillin and lactosurcose. penicillin G acylase retained its enzymatic activity at 88% and glycosidase at 92.8%, both after ten cycles of use. Lactosucrose was synthesized with a yield of 142 g L^{-1} (281.5 mM) for a total of 24 hours of reactor operation, and 68 g L^{-1} (186 mM) amoxicillin were produced in 260 min of operation, proving the excellent operability of the 3D-printed frames.

Another example of a novel modification protocol on 3D-printed surfaces is that of Sriwong and Matsuda (2022), who applied polydopamine (PDA)-coated 3D-printed materials for continuous flow biocatalysis.[26] Dopamine is an important compound in chemical biology and materials science because it shows intrinsic adhesiveness towards many different material surfaces, on which it attaches as a chemically reactive PDA priming layer. Its intrinsic reactivity towards, *e.g.*, thiols and amines, acts as a platform for secondary reactions for specific surface functionalization. The researchers here used thermoplastic polypropylene as an inexpensive material that is chemically stable towards a range of organic solvents. The enzyme of choice was an acetophenone reductase from *Geotrichum candidum* (GcAPRD), and the system was applied for asymmetric ketone reduction in a continuous flow mode. Both batch and microfluidic reactors were designed, going from 1.5 cm to 1.5 mm internal diameter. The batch reactors were used to optimize the immobilization protocol, and the best-performing protocol was elaborated for microfluidics fabrication. A comparison between the batch and microreactor systems revealed that higher immobilized protein per area could be achieved with the microfluidic system providing with an efficient use of materials surface for biomolecular interactions. The versatility of the 3D printing technology offered the opportunity to improve the system performance by designing and testing

Table 1 3D-printed reactors, reactor matrices, and reactor apparatus for flow biocatalysis

Description	Scale	Technique	Material	Enzymes	Comments	Ref.
Chemically surface-modified 3D-printed reactor	Milli-scale	Selective laser sintering (SLS)	Nylon 6 (fossil based)	ω-Transaminase ATA117	• Well-plate printed of the same material as the reactor for optimization of immobilization strategy • Remarkable activity and stability in flow, a total of 105 cycles of use	24
Chemically surface-modified 3D-printed reactor with integrated sphere-shaped scaffolds	Milli-scale	Fused deposition modeling (FDM)	Carbon-reinforced polylactic acid (C-PLA) (biobased)	Penicillin G acylase from *Providencia rettgeri* Protease WQ9-2 Glycosidase NJEM01 Lipase YCJ01	• Different enzyme classes immobilized with the same protocol • Good operability proved with lactosucrose and amoxicillin synthesis under continuous flow	25
Polydopamine-coated 3D-printed batch and microfluidic reactors	Milli-scale	Fused deposition modeling (FDM)	Polypropylene (fossil based)	Acetophenone reductase from *Geotrichum candidum*	• Novel surface modification protocol for 3D-printed materials • Immobilized acetophenone reductase in microfluidic reactors produced higher (*S*)-1-phenylethanol than previously reported yield with free enzyme	26
Chitosan-coated 3D-printed microreactor	Micro-scale	Fused deposition modeling (FDM)	Polylactic acid (biobased)	Laccase from *Trametes versicolor*	• Spectroscopic characterization revealed the degree of surface enrichment • Total turnover number of 4 386 000 for hydroxytyrosol conversion under continuous flow	27
Chitosan-coated 3D-printed microreactor	Micro-scale	Fused deposition modeling (FDM)	Polylactic acid (biobased)	Lipase from *Candida antarctica*	• 3D-printed material compatible with deep eutectic solvents (DES) for biocatalysis in non-conventional media • Exceptional stability under different conditions and incubation in DES	28
ZIF-8 modified 3D-printed micromixer	Micro-scale	Stereolithography (SLA)	Urethane methacrylate-based resin (clear resin V4) (fossil based)	Carbonic anhydrase from bovine erythrocytes Formate dehydrogenase from *Candida boidinii*	• Co-immobilization and domino immobilization approaches investigated • Almost 10 times increased yield for formic acid compared to conventional bubble column	29
3D-printed packing material for reactors	Milli-scale	Selective laser sintering (SLS)	Polyamide 12 (PA12) (Fossil based)	Phenolic acid decarboxylase from *Mycobacterium colombiense*	• Ferulic acid (FA) decarboxylation to 2-methoxy-4-vinylphenol (MVP) with *in situ* extraction of MVP with an organic solvent • 85% conversion in the first hour of reaction, 83% of the product extracted in the first 15 minutes of operation	30
3D-printed supports for enzyme immobilization as reactor inserts	Micro-scale	Stereolithography (SLA)	Ceramics	Phenolic acid decarboxylase from *Bacillus subtilis*	• Lattice structure with high surface area, reaching 58% immobilization yield and 6.02 U g^{-1} enzymatic activity • The decarboxylation of coumaric acid to vinylphenol reached a STY of 39.21 g $(L\ h)^{-1}$, outperforming previous reports by 8-fold	31

Table 1 (*Contd.*)

Description	Scale	Technique	Material	Enzymes	Comments	Ref.
Adapted reactor design with incorporated textile-immobilized biocatalyst	Milli-scale	Fused deposition modeling (FDM)	Transparent polyester copolymer (fossil based)	Peroxidase MaxiBright®	• Compartmentalized membrane-type reactor with low and continuously increasing concentrations of the inhibiting substrate • Yields under continuous flow improved by a factor of 30 compared to reactions in flasks	32
3D-printed interfacial device	Milli-scale	Fused deposition modeling (FDM)	Acrylonitrile-butadiene-styrene (ABS) (Fossil based)	Carbonic anhydrase from bovine erythrocytes	• The flotation level of the floating units was easily controlled by changing the void volume of the 3D models • The highest interfacial CO_2 conversion was obtained when the CA fibers were located right at the air–liquid interface	33

different reactors, and thus investigate the optimum enzyme immobilization yield, bioreactor area per volume, and continuous flow operation. As a result, 12.5 Units of immobilized enzyme on 3D-printed microfluidic bioreactors produced 43.2 mg of (*S*)-1-phenylethanol with >99% ee, while the previously reported milliscale reaction gave 98 mg of product, catalyzed by 50–250 Units of free enzyme, with up to >99% ee.

2.1.2 Micro-scale reactors. Aiming at a greener approach, Gkantzou *et al.* (2022) proposed a different modification protocol for 3D-printed biocatalytic microreactors.[27] The printing material used for the reactors was natural PLA (without additives, commercially available under the tradename of PrimaValue™) and a chitosan-based surface modification protocol was followed for enzyme immobilization. The optimization of surface modification and enzyme immobilization was assessed using 3D-printed multi-well plates. The optimized surface modification protocols were then transferred to printed micro-scale reactors to enable the immobilization of laccase from *Trametes versicolor* in their interior walls. X-ray photoelectron spectroscopy studies also revealed the degree of surface enrichment of the modified 3D-printed scaffolds. Process optimization under continuous flow was performed in terms of enzyme concentration, operational stability, and flow pattern. The model substrate was hydroxytyrosol, an industrially relevant and well-studied olive oil extract. A total turnover number (TTN) of 4 386 000 was achieved, indicating the viability of the designed system for repeated use of the immobilized biocatalyst. The versatility of the proposed reactor was demonstrated with the continuous flow biotransformation of several phenolic compounds from edible sources, reaching high conversion efficiencies in only one hour of residence time with mild reaction conditions.

The same research group, in a next attempt, used this chitosan-modified 3D-printed microreactor to perform biocatalysis in deep eutectic solvents (DESs)-based media,[28] that have been previously described as efficient solvents for biocatalytic processes.[34] This time using lipase from *Candida antarctica*, the continuous flow concept was used to investigate biocatalytic characteristics of the immobilized lipase like enzyme concentration, continuous flow kinetics in the presence or absence of DESs, operational stability, and storage stability in 100 vol% DES. Notably, the modified reactors maintain their rigidity after exposure to 100 vol% DES, demonstrating the potential of biobased 3D-printed materials for use with alternative solvents. Further findings were the solvent stabilizing effect on enzymatic activity, even at 100 vol% DES concentration, the 90% residual activity of the immobilized enzyme at 4 °C after two months of storage, and that the presence of the DES betaine : glycerol in the reaction system improved the apparent kinetic constant ($K_{M,app}$) of the enzyme greatly. The enzyme-microreactor system retained 53% of its activity after 30 days of storage in 100 vol% DES at 60 °C, while it got completely deactivated when stored in buffer solution. The study also exhibits a continuous flow transesterification reaction to produce glyceryl ferulate, a hard-to-obtain natural antioxidant, showing higher productivity than the batch reaction with a commercially available immobilized enzyme preparation.

2.1.3 Micromixers. Passive micromixers work in principle by following the change in structure along the channel length achieving enhanced mixing. Their simple operation has led to their incorporation into several microscale processes.[35] The investigation has been conducted on the mass transfer characteristics of different internally shaped micromixers for the absorption of CO_2 in water and alkaline solutions, revealing that the mass transfer coefficients were one or two orders of magnitude higher than that of commonly used contactors like bubble and packed-bed column reactors.[36,37] Chai *et al.* (2021) applied this concept to demonstrate a biocatalytic micromixer for the conversion of CO_2 to formic acid.[29] The micromixer was fabricated using the stereolithography (SLA)-based 3D printing technology with a commercial transparent urethane methacrylate-based resin (Clear Resin V4). This approach allowed for different internal structure designs to assess the best-performing mixer. The interior of the microchannels was chemically modified, and a biomineralization method was followed to immobilize the enzymes of interest on a ZIF-8 thin film. For the cascade reaction, carbonic anhydrase (CA) and formate dehydrogenase (FDH) were elaborated. The biocatalytic concept was adopted by co-immobilizing the enzymes in a single microchannel and by a domino approach, immobilizing each enzyme in a different micromixer and interconnecting them. A simulation study of the concentration distribution of liquids within the micromixer showed almost 100% mixing efficiency across different Reynolds (Re) numbers (from 4 to 25), making the system suitable for applications requiring high reaction control. The system was also microscopically and spectroscopically characterized proving the efficiency of the surface modification protocol and the enzyme immobilization in the ZIF microstructures. Different two-phase flow patterns were investigated, and the effect on the biocatalytic activity was assessed. A combination of bubbly/slug flow was found to be the ideal condition for sufficient product yield, while the two different immobilization approaches, co- or domino immobilization, did not seem to produce significantly different results. However, the independently immobilized systems can provide important information for the reaction, like the rate-limiting step. The optimum system produced formic acid at a rate of 0.97 $mol_{formic\ acid}$ $(kg_{enzyme}\ h)^{-1}$. A corresponding system in a conventional bubble column showed a production yield of 0.1 $mol_{formic\ acid}$ $(kg_{enzyme}\ h)^{-1}$, despite the significantly higher immobilization yield in the column than in the micromixers, 87% and 22%, respectively. Concluding, this study gives the reader a perspective on the potential of 3D printing in designing modular devices with specific functions for cascade enzymatic reactions on the microscale.

2.2 3D printing the reactor matrices

An example of 3D-printed packing material for reactors was developed in the work of Büscher *et al.* (2020).[30] This study describes a tailor-made structure, acting as an enzyme immobilization matrix and an extraction-phase distributor at the same time. The motive of the study was the precise control of geometry that can directly affect the flow behavior of an organic extraction phase and can be readily achieved with additive manufacturing. Indeed, 3D printing allowed the researchers to investigate different reactor internal structures, and hence improve their influence on extraction relevant parameters, like the surface-to-volume ratio, the droplet size, and the residence time. Selective laser sintering (SLS) was chosen as a 3D printing approach that offers high surface roughness which can be beneficial for enzyme immobilization. Phenolic acid decarboxylase (PAD) from *Mycobacterium colombiense* was immobilized on a matrix material made of 3D-printed polyamide 12 located in a glass column reactor system. The aim was to perform ferulic acid decarboxylation to 2-methoxy-4-vinylphenol (MVP), implementing *in situ* extraction of MVP with an organic solvent. PAD has been shown to undergo product inhibition under the conditions ($K_{i,MVP}/K_{M,FA} = 0.06$),[38] so the importance of *in situ* product extraction is underlined by the authors. This type of reactor had been previously used for ferulic acid bioconversion. Still, it was the first time that a study focused on improving the mass transfer of the reaction product to the organic extraction phase. By doing so, 85% conversion was observed in the first hour of reaction, while 83% of the product was extracted in the first 15 minutes of operation. The newly developed matrix material also contributed to an enhanced surface area, compared to previous studies, for an increased enzyme loading that is substantial for conversion efficiency. Overall, this study is a good example of bioprocess intensification by combining biocatalysis and *in situ* extraction within a countercurrently operated reactor utilizing 3D-printed packing material.

Also, the work by Valotta *et al.* (2021)[31] locates in the field of 3D printing reactor inserts for continuous flow biocatalysis. PAD from *Bacillus subtilis* was the enzyme of choice, this time for the decarboxylation of coumaric acid to vinylphenol. The enzyme was covalently immobilized on the 3D-printed support structures after proper support functionalization to introduce reactive groups on its surface. Different geometries of the inserted structures were assessed in terms of flow behavior with a residence time distribution (RTD) approach. Ceramics were used as the 3D-printed material in a standard vat photopolymerization (VPP or commonly SLA) printing technique. The choice for ceramics, instead of standard 3D-printable polymer resins, resulted in great enzyme-carrier compatibility, demonstrated by long-term activity and stability. The 'freedom of design' offered by 3D printing resulted in an optimum lattice structure with a high surface area, reaching 58% immobilization yield and 6.02 U g^{-1} enzymatic activity. The continuous flow bioconversion was performed in an automated screening set-up for the optimization of the reaction. 3D printing was employed also for the fabrication of static mixers to provide the system with a feed stream of uniform concentration before it reaches the reactor inlet. Applying a design of experiments (DoE) approach with this setup, a space-time yield (STY) of 39.21 g $(L\ h)^{-1}$ was reached, outperforming the previously reported by eight-fold. The authors claimed that the possibility to easily design and manufacture interchangeable inserts *via* 3D printing allows for rapid adaptation to the reaction needs, thus achieving optimal process conditions. This work was also a good example of realizing functional low-cost alternatives to

analytical equipment that increased the level of process understanding.

3. 3D printing the biocatalysts

3D printing of the biocatalyst requires formulating it with support material, typically hydrogel-forming polymeric pregels, and using this mixture as a 3D-printable ink or resin (Fig. 3). Bioinks and bioresins are obtained when living cells are used as the biocatalyst and mixed in the polymeric pregel. The resulting 3D printing process is called 'bioprinting'.[39] It involves assembling cellular bio-entities *via* extrusion-based printing of one or multiple bioinks or, less commonly, by crosslinking the bioresin layer-by-layer *via* SLA- or digital light processing (DLP)-based printing to create bio-engineered living materials. In contrast, formulating active enzymes into a polymeric pregel without cells results in a bioactive and/or biocatalytic ink or resin to 3D-print bioactive scaffolds or matrixes for biomedical applications or biotechnological processes. The striking argument for 3D printing of the biocatalyst compared to a simple casting is the potential to easily control the 3D shape of the resulting biocatalytic matrix as well as the spatial distribution and/or local concentration of the biocatalyst in a modular fashion, including multiple-enzyme or cellular coculture systems for cascade biotransformations.

3.1 3D printing of cells

For whole-cell biocatalysis, only a few examples have been described so far involving yeast cells to develop living materials for biocatalytic process intensification or bacteria-algae co-cultures for bioremediation processes.[40–42] However, with the continuous bioprinting advancements in the field of tissue engineering and regenerative medicine, naturally focusing on mammalian cell printing, the dawning of bioprinted whole-cell catalysts can be foreseen with a shift towards prokaryotic cell printing.[43] A pioneering example in that direction was reported in 2021 by Duraj-Thatte *et al.*,[44] who established a 'microbial ink' and printed functional living materials from the shear-thinning hydrogel based on fibrin-inspired nanofibers produced by genetically engineered *E. coli.* The inks contained different genetically engineered *E. coli* to demonstrate their functionality and application diversity with, *e.g.*, chemically-induced, on-demand production and extracellular secretion of azurin as a potential anti-cancer drug. Similarly, Cui *et al.* established the extrusion-based 3D printing of hyaluronic acid-producing *Streptococcus zooepidemicus* in a conventional photocrosslinkable gelatin-based matrix often used for mammalian cell printing.[45] They demonstrated the benefits of 3D printing for the yield and production efficiency of the bacterial metabolite hyaluronic acid due to improved mass transfer within bacteria-containing hydrogel grid structures with optimized geometry and high surface-to-volume ratios compared to bulk gels. Because extrusion-based bioprinting has virtually the same ink requirements for eukaryotic and prokaryotic cells in terms of overall biocompatibility, mechanical integrity and stability of printed structures, and reduction of shear stress relative to the cell membrane, many of the inks previously developed for mammalian cells can also be used for prokaryotes. Besides extrusion- also SLA-based bioprinting has been demonstrated to be applicable to print bacterial cells.[46]

In general, whole-cell biocatalysis is especially advantageous for cofactor-dependent reactions since the inherent presence of cofactors that are generated by the host cell and the ease of their recycling greatly improve the economics of the process.[47] The potential to convert cheap and abundant raw materials in multistep reactions into valuable chemicals without time- and material-intensive enzyme isolation and purification, thus often simplifying both up- and downstream processing, contributes to their economic attractivity. Adverse substrate transfer limitations across the cell membrane can be overcome by printing surface-engineered cells, which display heterologous enzymes extracellularly.[48] Hence, with the many powerful tools available nowadays to engineered both cells and inks, rapid advances in the field of bioprinting sustainable living materials for whole-cell biotransformations in continuous flow systems are to be expected.

3.2 3D printing of enzymes

When it comes to bioactive cell components, *i.e.*, enzymes, we can find more literature reports, some of which also dealing

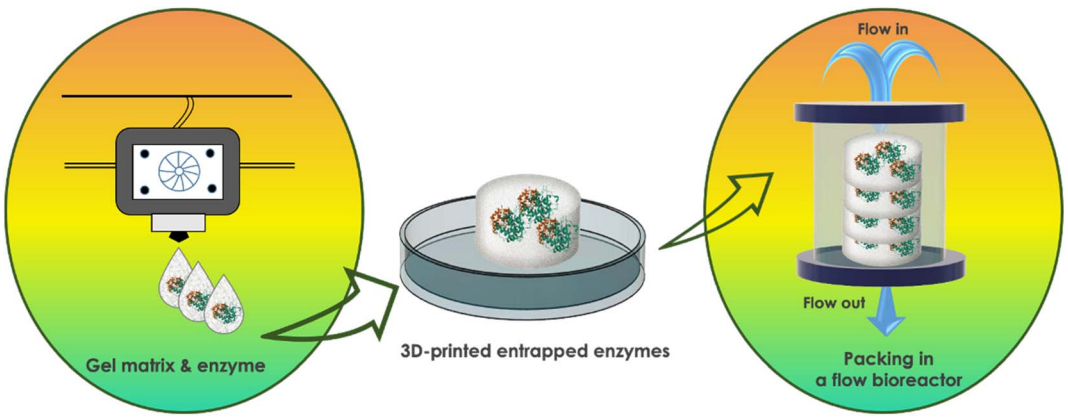

Fig. 3 3D printing of biocatalysts for flow biocatalysis.

Table 2 Representative examples of 3D-printed biocatalysts

Biocatalysts	Technique	Material	Comments	Ref.
Alcohol dehydrogenase from *Lactobacillus brevis*, benzoyl formate decarboxylase from *Pseudomonas putida*, β-galactosidase from *Aspergillus oryzae*	Pneumatic extrusion-based 3D printing	Poly(ethylene glycol) diacrylate (PEG-DA)	Advantages and limitations of 3D-printed reactors with entrapped enzymes for biocatalysis	53
β-galactosidase from *Aspergillus oryzae*	Pneumatic extrusion-based 3D printing	Poly(ethylene glycol) diacrylate (PEG-DA) with viscosity-enhancing additives Laponite RD, Deuteron XG, Bentone MA	Development of a 3D-printable hydrogel material for long-term biocatalytic applications	54
Laccase from *Trametes versicolor*	Extrusion-based bioprinting	Sodium alginate-acrylamide hydrogel with hydroxyapatite additive	Biodegradation of the phenolic compound *p*-chlorophenol	55
β-Galactosidase	3D jet writing	Poly(ethylene glycol) (PEG) and poly(acrylic acid) (PAA)-based hydrogels mixed with poly(ethylene glycol) diacrylate (PEGDA)	Evaluation of enzyme activity, reactants transport capacity, and long-term stability after immobilization in a hierarchically defined scaffold	56
Glucose oxidase, catalase	Extrusion-based bioprinting	Sodium alginate/ polyacrylamide/ hydroxyapatite (SA/PAM/HA) hybrid interpenetrating polymer network (HIPN) hydrogel	One-pot multi-enzyme immobilization for the synthesis of gluconic acid	57
Tyrosinase	Extrusion-based bioprinting	Gelatin-methacryloyl (GelMA)-collagen hydrogels	Exploration of the dual role of tyrosinase: hydrogel cross-linking and skin regeneration process	58
Cellulase	Pneumatic extrusion-based 3D printing	Cellulose nanofiber (CNF) reinforced chitosan (CHI) hydrogels	Controlled enzyme release for the inherent biodegradation of implantable biomaterials for tissue engineering	59
Yeast cells, and *Bacillus subtilis* co-entrapped with *Chlorella vulgaris*	Extrusion-based 3D printing	cucurbit[8]uril (CB[8])-mediated host–guest complex and methacrylate-based photochemically double-crosslinked dynamic bioink based on hyaluronic acid	Yeast-laden materials for the fermentation of glucose to ethanol and, bacteria-microalgae cocultured living materials system for bioremediation	42
Baker's yeast (*Saccharomyces cerevisiae*)	Pneumatic extrusion-based 3D printing	Polyethylene glycol dimethacrylate (PEGDA) with nanocellulose filler	Glucose fermentation	40
Yeast cells (*Saccharomyces cerevisiae*)	Direct-write 3D printing	F127-dimethacrylate (F127-DMA)-based hydrogel	Bioethanol production	41
Amine dehydrogenase variant (AmDH-v1), formate dehydrogenase (Cb-FDH)	Stereolithography	Agarose gel	Reductive amination of benzaldehyde in continuous flow	60
Ketoisovalerate decarboxylase (KIVD) mutant from *Lactococcus lactis* Alcohol dehydrogenase (ADH) from *Alicyclobacillus acidocaldarius*	Pneumatic extrusion-based 3D printing	Agarose hydrogel	Two-step biotransformation of ketoisovalerate (KIVD-catalyzed decarboxylation) into isobutanol	52
Phenacrylate decarboxylase from *Enterobacter* sp.	Pneumatic extrusion-based 3D printing	Agarose hydrogel	Continuous flow production of 4-hydroxystilbene from *p*-coumaric acid	61

with flow biocatalysis. A list of the 3D-printed biocatalysts so far and their applications is presented in Table 2. Previous review papers have also described the advances in biocatalysts incorporation in 3D-printable matrices. Focusing on the 3D-printed enzymes, the idea is based on the search for new immobilization carriers since conventional carriers, in the form of beads and granules for packed-bed reactors, do not allow for complex 3D structures with the desired shapes, sizes, and physical properties needed to produce customized reactor components for biocatalytic applications.[49] Simple one-step fabrication methods incorporate enzymes in the printing material (entrapment), resulting in high enzyme activity retention due to the mild non-covalent immobilization conditions. However, careful consideration of enzyme compatibility with the raw printing materials is needed since printability and enzyme activity are directly influenced. The advantages, challenges, and future perspectives of 3D printing of enzymes entrapped in hydrogels are presented in recent reviews.[49,50] An extrusion-based 3D printing technique is commonly employed for polymer-based enzyme formulations, which physically gel upon, *e.g.*, temperature change or covalently crosslink upon irradiation of the printed structures in the presence of a suitable photoinitiator. Physical thermogelation is generally advantageous over chemical photocrosslinking in biocatalyst printing, as it does not produce radicals potentially affecting the encapsulated enzyme's structure and activity or require post-print processing steps. Furthermore, compared to living tissue printing, the requirements for printing resolution are generally lower in biocatalyst printing as it hardly affects the performance of the biocatalytic process. Thus, the often-encountered limited printing resolution of extrusion-based printers – particularly with thermogelling materials – compared to resin-based SLA printers can be neglected for most matrix-embedded biocatalyst prints. However, temperatures up to 60 °C may be needed in extrusion-based printing, again particularly with thermogelling inks, to ensure the optimal ink viscosity for an efficient printing process. Thus, for such applications, a high thermostability of the used enzymes is a prerequisite.[51] In the following paragraphs, we will examine some examples from the literature that have employed this immobilization method to develop continuous flow biocatalytic reactors.

Maier *et al.* (2018) demonstrated the development of biocatalytic flow reactor cartridges composed of only the enzyme and an inexpensive agarose matrix that can be produced on-site, on-demand, and are biodegradable after use.[52] Esterase (EstII) and alcohol dehydrogenase (ADH) from thermophilic organisms and an engineered decarboxylase from a mesophilic source were evaluated as the biocatalytically active ink's components. It is worth here to mention that the authors used the term 'bioink' for the described application of isolated enzymes, which we herein prefer to call 'biocatalytically active inks'. After the preparation of the enzyme-containing inks by mixing the buffered agarose polymer solution with the respective purified enzyme at elevated temperature, their activity in fresh and temperature-treated gelled samples was analyzed. Therefore, the samples were incubated at 60 °C, simulating the temperature of the printer shell. Their residual EstII-catalyzed de-esterification activity towards a fluorescein derivative and their ADH-catalyzed reduction to yield isobutanol were analyzed in comparison with untreated controls. It was found that the enzymes could be incubated at 60 °C without significant activity loss – around 80% residual activity was detected after 240 min. Thus, after the 15 min printing process, the enzymatic activity of 85 ± 9% for ADH and 96 ± 12% for EstII was maintained.

The proof-of-concept under flow conditions was demonstrated with a mesophilic enzyme designed with protein engineering to broaden the applicability of the method to non-naturally thermostable variants. The enzyme of the first step of the cascade was the engineered ketoisovalerate decarboxylase (KIVD_mutant). A recovered activity of 36 ± 7% was detected after the printing process for the decarboxylation reaction of ketoisovalerate at 60 °C. Under flow conditions in the first 40 min of operation, the 3D-printed engineered enzyme reached 40% product yield in transforming ketoisovalerate to isobutyraldehyde within the agarose matrix. A flow reactor system was later used for the two-step biotransformation of ketoisovalerate into isobutanol catalyzed by KIVD_mutant and ADH 3D-printed enzyme-agarose disks in a cascade fashion. Isobutanol yield was found to be ADH dependent, as adding more ADH disks to the system increased the final product concentration. The authors argued that the 3D-printed hydrogel structures enabled the direct flow of the substrate solution inside the reactor and estimated the diffusion into the gel to reach a rate of 100 μm s^{-1}. Data were also provided for the enhanced tolerance of the agarose-entrapped enzymes towards organic solvents, proving the agarose matrix's significant protection of the enzymes. Molecular weight-dependent enzyme leaching from the agarose gel matrix was observed and quantified with western blot analysis of the outflow. This revealed a maximum enzyme elution of 0.9% for ADH, and 0.7% for KIVD per mL flow-through. The proposed setting could withstand operational volumes of up to 70 mL of product. The study showed that this 3D printing approach allowed for the rapid prototyping of the desired structures, enabling systematic screening of construction parameters and optimization of reactor performance by modulating the shape and surface/volume aspects, utilizing inexpensive materials and simple immobilization methods.

In the subsequent research from the same group, Peng *et al.* (2019) demonstrated the 3D printing of biocatalytic gel modules to be integrated into a chemoenzymatic reaction cascade that would produce 4-hydroxystilbene, a pharmacologically relevant compound.[61] Different phenacrylate decarboxylases were screened for their thermostability since 60 °C was needed for the extrusion-based 3D printing process (initial heating step at 60 °C for 15 min). The enzyme variants were mixed with 2-hydroxyethyl agarose solutions to formulate the biocatalytically active inks and print the gel-based reactor modules. After integration in a flow reactor system, outflow analysis revealed one enzyme variant with higher thermostability and product yield than the others. It is important to notice, though, that a time-dependent decrease in the conversion rate was observed and was related to the leaching of the encapsulated enzyme, as previous studies had similarly shown. After an optimization

process, an efficiency of 98% over 40 hours of use was obtained. A scale increase by numbering-up was also demonstrated, leading to the conversion of 35 mg *p*-coumaric acid in a total volume of 211 mL with an average total turnover number (TTN) of 590 (4-vinyl phenol molecules per enzyme). The outflows were collected, and an isolated yield of 54% was obtained. 4-Hydroxystilbene was produced in a yield of 15% after a chemocatalytic step. The authors conclude that the proposed method can be elaborated to easily screen new enzyme classes compatible with 3D bioprinting. Also, the manufacturing process facilitated the modularity and scalability of the reactor system, introducing new enzyme classes into flow reaction systems.

Croci *et al.* (2022) approached the matter from a different perspective. They compared the hydrogel-based 3D-printed enzymes with conventional immobilization techniques – affinity or covalent – on commercial bead carriers in batch and continuous flow systems.[60] The application focused on producing α-chiral amines, found in 40% of the commercialized optically active pharmaceutical intermediates. The reductive amination of benzaldehyde to benzylamine was performed by co-immobilizing a novel engineered amine dehydrogenase variant (AmDH) and formate dehydrogenase (FDH) as an NADH-recycling enzyme. For comparison with the commercial carriers, cation-affinity binding with EziG (preloaded with Fe^{3+}) and Purolite (pre-loaded with Co^{2+}) beads, or Sepabeads (EC-EP/s) and Relizyme (113/s and 403/s) for epoxide-amine covalent attachment were used for AmDH and FDH co-immobilization. Several issues were encountered with the commercial beads, from low product yields in some cases to substrate adsorption and enzyme leaching resulting in the incompatibility of the tested methods for establishing a reductive amination process in flow. Therefore, the researchers developed an 'agarose gel reactor' of pre-defined geometry and proposed a way to enable the enzyme entrapment at a lower temperature (40 °C) to be generally applicable also with mesophilic enzymes. For this reason, 3D-printed enzyme-agarose hydrogels were cast at 40 °C in a 3D-printed mold made of methacrylate-based resin. Different reactors and reactor channels were tested without reprinting the enzyme-containing module. Sufficient stability and reusability of the enzyme-loaded gel matrix were observed. An optimized process was performed over the course of 120 hours with 30 mM substrate concentration, and the system afforded 47% analytic product yield, of which 34% was isolated by extraction. Finally, the authors demonstrated an improved efficiency of the amination reaction in terms of product formed per amount of biocatalysts by implementing co-entrapped AmDH/FDH enzymes in a continuous flow cascade reaction. Detailed tables for a direct comparison of the amination reaction in the proposed system with previously established batch systems were also provided, highlighting a TTN of 3239 in flow *versus* the previously reported value of 943.

4. 3D printing of reaction apparatus

Apart from directly applied biocatalytic modules, 3D printing has also shown great potential in designing the desirable apparatus to facilitate the biocatalytic process. Researchers generally prefer to flexibly design and implement their accessories and devices to their overall system needs by modifying and adjusting in a 'trial-and-error' mode. In contrast, working with fixed commercial products and trying to fit them into the respective system is often process-limiting and laborious. The preferable 3D printing technique here is fused deposition modeling (FDM) because of the quick design and modular parts' mechanical robustness. Due to the vast choice of thermoplastic materials, the mechanical and chemical stability of the final additively manufactured product can easily be adjusted to and matched with the requirements of the desired application. In literature, we can find numerous examples with 3D-printed apparatus for fluidic applications:[62] molds and scaffolds as an indirect approach to develop fluidic networks, complex structures and devices like microvalves, pumps, and multiplexers, cell sorters for cell biology applications, microfluidic tools for immunodetection, or even point-of-care (POC) devices manually operated. An exciting approach by Hou *et al.* (2021) proposed the automatic generation of 3D-printed reactionware for chemical synthesis through a computational platform that predicts and generates the specific reactor (tailored for the desired geometry, flow profile, dimensions, or also considering the material choice) fitted for the target chemical reaction.[63]

In the field of flow biocatalysis, Wunschik *et al.* (2020) adopted the 3D printing technology to develop a reactor module for the enzymatic epoxidation of cyclohexene by a textile-immobilized peroxidase.[32] This module would host the biocatalytic textile to realize a continuous flow process. The shift from a batch to a continuous process in this work was performed as a tool to tackle enzyme inhibition by the substrate hydrogen peroxide. At the same time, it also allowed for a modular design to fit into the specific process needs. Moreover, continuous product extraction could be performed while maintaining maximum biocatalyst activity.

For this reason, the FDM approach was adopted with a transparent polyester copolymer filament based on terephthalic acid to fabricate a two-compartment reactor. The upper chamber was filled with cyclohexene as a substrate, and the bottom part with acetonitrile as an extraction solvent. Peroxidase enzyme was immobilized on the textile and placed at the phase boundary. Cyclohexene oxidation occurred at the textile upon influx of hydrogen peroxide from the cyclohexene overlaying aqueous phase. The formed epoxide was quickly removed by extraction to the organic phase on the other compartment side of the reactor. Hence, a membrane-type reactor was developed with a low and continuously increasing concentration of the inhibiting substrate (hydrogen peroxide). Notably, the yields obtained in the developed reactor were enhanced by a factor of 30 compared to the reactions performed in flasks. The authors conclude that only a conjunction of immobilization technique and reactor design can lead to a new economic chemo-enzymatic reaction route.

In a different approach, Kim and colleagues (2020) demonstrated the usefulness of AM-enabled design freedom for an interfacial device that could facilitate the biocatalytic CO_2

conversion at a gas–liquid interface.[33] The enzyme of interest here was carbonic anhydrase (CA), immobilized onto electrospun fibers as a promising carrier for CA that was previously proved to enhance enzyme stability significantly.[64] Although immobilized CA has already been utilized in previous studies, the advancement of this work was the interfacial positioning of the biocatalyst, resembling the natural CO_2 sequestration. Such precise positioning could be effectively realized using 3D printing technology that allowed for the design of a density-adjustable platform consisting of biocatalytic and floating units. FDM printing technique with a widely used acrylonitrile-butadiene-styrene (ABS) copolymer filament was employed. The flotation level of the floating units was easily controlled by changing the void volume of the 3D models. For the bioreactor part, different modules for each step of the reaction were assembled, and the position of the immobilized CA fibers was investigated. The highest interfacial CO_2 conversion was obtained when the CA fibers were located right at the air–liquid interface (flotation level 0 cm). A gradual performance decrease was observed at higher flotation levels, reaching the range of non-enzymatic processes at levels −2 and −2.5 cm. This way, it was proved that enzymatic CO_2 conversion primarily occurs at the air–water interface, suggesting the importance of adequately positioning immobilized CA or other enzymes for successful interfacial biocatalysis. Adopting the proposed 3D-printed interfacial device could facilitate the control of the spatial positioning at the biphasic interface simply by adjusting the density of the floating enzyme carrier.

5. Sustainability assessment

It is worth to examining how we can address the sustainability and efficiency by the design of 3D printing for flow biocatalysis covering (i) materials and (ii) time-to-process. The advantages

Table 3 Representative examples of materials used in flow biocatalysis applications in 2020–2023

Material	Flow technology	Productivity	Ref.
Cellulose microcrystalline Avicel® PH-101	Immobilized protein preparations packed into an Omnifit column	0.37 $g_{product}$ L^{-1} h^{-1}	78
Agarose epoxy beads, polytetrafluoroethylene (PTFE)	Immobilized enzymes preparations packed into a custom-made PTFE reactor	19.31 $g_{product}$ d^{-1} L^{-1}	79
Poly(methyl methacrylate) (PMMA)	Crude-enzyme hydrogel monolithic microreactor	46.3 $g_{product}$ L^{-1} h^{-1}	80
Hydrogel comprising dimethacrylate-functionalized Pluronic F127 (F127-DMA) and sodium alginate (Alg)	Packed column	74.6% dye degradation	81
Purolite resin beads	Immobilized enzyme beads packed into an Omnifit column	10.6 $g_{product}$ g_{enzyme}^{-1}	82
Magnetic nanoparticles, PTFE	Magnetic nanoparticles loaded tube microreactor	11.6 mmol L^{-1} h^{-1}	83
Commercially available streptavidin (STV)-coated magnetic particles (MB), PMMA	Straight channel microreactor made of PMMA packed with magnetic particles with immobilized enzyme	28.9 mol L^{-1} h^{-1}	83
Epoxide microparticles, PTFE	Reactor chamber made of PTFE packed with microparticles with immobilized cells (all-enzyme hydrogel particles)	18.8 $g_{product}$ L^{-1} d^{-1}	84
Perfluoroelastomer (PFE)	Segmented-flow PFE coil microreactor with whole-cells	12.5 $g_{product}$ L^{-1} h^{-1}	85
Carbon particles, glass beads	Omnifit glass column packed with carbon and glass beads with immobilized enzymes	11.2 $g_{product}$ L^{-1} h^{-1}	86
Alginate hydrogel, glass, silicon, Teflon	Glass-silicon-glass microreactor in a Teflon housing loaded with alginate hydrogel and enzyme mixture	52.94% and 33.61% conversion yields for two different products	87
Perfluoroalkoxy (PFA)	Flow reactor and Y-mixer made of PFA loaded with commercially available immobilized enzyme preparations	85.2% main product yield	88
Multi-wall carbon nanotubes, quartz	Multi-wall carbon nanotube lined quartz tubes with surface immobilized enzyme	38.7 $g_{Product}$ L^{-1} h^{-1}	89
Borosilicate glass, zinc oxide (ZnO) nanowires	Glass capillaries with *in situ* grown ZnO nanowires and surface immobilization of enzyme	0.29 $mg_{product}$ min^{-1} mg_{enzyme}^{-1}	90

that flow biocatalysis can bring alone are not covered since this has been extensively reviewed before, as highlighted in the Introduction.

5.1 Materials

To start with, a life cycle assessment of the materials used in the most common 3D printing technologies has been described in several review articles, while 'case studies' are currently being conducted to assess the recycling and reusing potential of these materials. There are some analytic reports[3,4] on sustainability aspects of additive manufacturing that the reader can be redirected to. More specifically, there have been detailed references for (i) recyclable and biobased photoresins,[2] (ii) recycled and biodegradable filaments,[65] and (iii) sustainable hydrogels that have been very recently described in a dedicated book.[66] For example, PLA (bio)degradation and recycling has been under intensive study[67–70] since it is the most commonly used material in the 3D printing world. Thus, chemical,[71] mechanical,[72] and biological methods[73,74] have already been described, while there are also companies specializing in PLA and other 3D-printed filaments recycling. Shredding and re-extruding are also widely applied by individuals and companies (Filabot, Dyze Design, *etc*). Table 3 reports recent examples of existing flow technologies and their materials for biocatalytic applications. These data suggest plenty of room for 3D-printed materials to invade and change the sustainability aspects of currently applied flow technologies. Commonly used polymer materials like PMMA and PTFE have already entered the market in 3D-printable forms. Regarding hydrogels for enzyme- or cell entrapment, we already highlighted in the previous sections the contribution of 3D printing that several laboratories increasingly elaborate on. When it comes to the most common material in terms of all kinds of reactors, glass is already on the market for 3D printing, and maybe such materials could already start to replace some traditionally manufactured glass microstructures.[75–77]

5.2 Time-to-process

Flow biocatalysis meets essential requirements of sustainable processes, like high reusability of the systems, time and cost-efficiency with low reaction times and small-scale equipment, and minimal waste production.[7] Incorporating additive manufacturing in the establishment of biocatalytic flow systems has a strong potential to enhance these aspects further. In chemical engineering, including the field of biocatalysis in flow systems, highly sophisticated systems are typically required to establish precise process control and reassure the biocatalyst's longevity. We saw in this review examples of substantial productivity enhancements when shifting to a continuous flow regime with the help of 3D printing. It can be predicted that the easy-to-adjust trait of this technology will be increasingly elaborated in future biocatalytic applications. Fluidic systems possess modularity, so there is a great need for accordingly modular accessories and reactionware that would fit a specific process. Moreover, the opportunity to 3D-print the enzyme, protected inside its scaffold, offers an alternative immobilization approach with promising results for a cost-effective and green process design.

6. Conclusion and future perspectives

In conclusion, it is foreseen that the principles of 'quality of design' and 'quality by control' could be applied since the combination of flow biocatalysis and additive manufacturing leads to automated and/or highly controlled processes. From design to implementation, the time and costs are constantly being reduced, framing not only innovative but also sustainable processes. The joined forces of materials science and bioprocess engineering will profit extensively regarding the tailor-made material design that provides the desired characteristics, including biodegradation and functionality. The targeted material–biomolecular interactions will pave the way for highly efficient continuous biocatalytic production. Additive manufacturing has undoubtedly changed scientists' way of thinking due to technology-enabled freedom of experimental design. Developing custom devices has now become an everyday practice for numerous laboratories, as the costs of this technology are getting consistently lower. It is important to note, though, that an important barrier to the industrial adoption of such processes is print-to-print inconsistency.[91] Reasons for this can be found in the differences between batches of materials and the inability of the 3D printing systems to couple the deposition parameters to the dynamic material properties. Scientists are already on their way to overcoming issues like this by adopting artificial intelligence (AI) to design closed-loop control systems and achieve optimum printing consistency.[92] This way, we can expect a broader implementation of highly intricate systems in chemical engineering sciences that would unlock tremendous potential for the future of biocatalytically produced compounds.

Author contributions

E. Gkantzou and S. Kara conceived the conception and design of this work. S. Kara was responsible for funding acquisition and project administration. All authors contributed to the writing of the original draft, reviewed, and edited the final draft, and agreed with the final version of the submitted manuscript.

Conflicts of interest

There are no conflicts to declare.

Acknowledgements

S. K. thanks the Independent Research Fund Denmark, PHOTOX-*f* project, grant no. 9063 00031B, for the grant funding. S. K. thanks the Ministry for Science and Culture for Lower Saxony for the Holen & Halten starting grant (grant no. 12.5-76251-17-9/20).

References

1 M. Touri, F. Kabirian, M. Saadati, S. Ramakrishna and M. Mozafari, *Adv. Eng. Mater.*, 2019, 21.
2 K. P. Cortés-Guzmán, A. R. Parikh, M. L. Sparacin, A. K. Remy, L. Adegoke, C. Chitrakar, M. Ecker, W. E. Voit and R. A. Smaldone, *ACS Sustainable Chem. Eng.*, 2022, **10**, 13091–13099.
3 E. M. Maines, M. K. Porwal, C. J. Ellison and T. M. Reineke, *Green Chem.*, 2021, **23**, 6863–6897.
4 E. Sanchez-Rexach, T. G. Johnston, C. Jehanno, H. Sardon and A. Nelson, *Chem. Mater.*, 2020, **32**, 7105–7119.
5 A. J. Capel, R. P. Rimington, M. P. Lewis and S. D. R. Christie, *Nat. Rev. Chem.*, 2018, **2**, 422–436.
6 J. Britton, S. Majumdar and G. A. Weiss, *Chem. Soc. Rev.*, 2018, **47**, 5891–5918.
7 L. Tamborini, P. Fernandes, F. Paradisi and F. Molinari, *Trends Biotechnol.*, 2018, **36**, 73–88.
8 P. De Santis, L.-E. Meyer and S. Kara, *React. Chem. Eng.*, 2020, **5**, 2155–2184.
9 P. Žnidaršič-Plazl, *Biotechnol. J.*, 2019, **14**, 1800580.
10 L.-E. Meyer, M. Hobisch and S. Kara, *Curr. Opin. Biotechnol.*, 2022, **78**, 102835.
11 G. Vernet, M. Hobisch and S. Kara, *Curr. Opin. Green Sustainable Chem.*, 2022, **38**, 100692.
12 S. C. Cosgrove and A. P. Mattey, *Chem.–Eur. J.*, 2022, **28**(13), e202103607.
13 A. J. Tušek, A. Šalić and B. Zelić, *Appl. Biochem. Biotechnol.*, 2017, **182**, 1575–1590.
14 A. Valotta, L. Malihan-Yap, K. Hinteregger, R. Kourist and H. Gruber-Woelfler, *ChemSusChem*, 2022, **15**, e202201468.
15 M. P. Thompson, I. Peñafiel, S. C. Cosgrove and N. J. Turner, *Org. Process Res. Dev.*, 2018, **23**, 9–18.
16 S. N. Chanquia, A. Valotta, H. Gruber-Woelfler and S. Kara, *Front. catal.*, 2022, 1.
17 V. Alphand, W. J. H. van Berkel, V. Jurkaš, S. Kara, R. Kourist, W. Kroutil, F. Mascia, M. M. Nowaczyk, C. E. Paul, S. Schmidt, J. Spasic, P. Tamagnini and C. K. Winkler, *ChemPhotoChem*, 2023, **7**, e202200325.
18 V. Sans, *Curr. Opin. Green Sustainable Chem.*, 2020, **25**, 100367.
19 K. M. Zentel, M. Fassbender, W. Pauer and G. A. Luinstra, *Adv. Chem. Eng.*, 2020, 97–137, DOI: **10.1016/bs.ache.2020.08.002**.
20 L.-E. Meyer, D. Horváth, S. Vaupel, J. Meyer, M. Alcalde and S. Kara, *React. Chem. Eng.*, 2023, **8**, 984–988.
21 T. Pose-Boirazian, J. Martinez-Costas and G. Eibes, *Macromol. Biosci.*, 2022, **22**, e2200110.
22 M. Romero-Fernandez and F. Paradisi, *Curr. Opin. Chem. Biol.*, 2020, **55**, 1–8.
23 G. Palmara, F. Frascella, I. Roppolo, A. Chiappone and A. Chiado, *Biosens. Bioelectron.*, 2021, **175**, 112849.
24 E. Peris, O. Okafor, E. Kulcinskaja, R. Goodridge, S. V. Luis, E. Garcia-Verdugo, E. O'Reilly and V. Sans, *Green Chem.*, 2017, **19**, 5345–5349.
25 J. Ye, T. Chu, J. Chu, B. Gao and B. He, *ACS Sustainable Chem. Eng.*, 2019, **7**, 18048–18054.
26 K. T. Sriwong and T. Matsuda, *React. Chem. Eng.*, 2022, **7**, 1053–1060.
27 E. Gkantzou, A. Skonta, A. Tsakni, A. Polydera, D. Moschovas, K. Spyrou, A. Avgeropoulos, D. Gournis, D. Houhoula and H. Stamatis, *J. Biotechnol.*, 2022, **350**, 75–85.
28 M. G. Bellou, E. Gkantzou, A. Skonta, D. Moschovas, K. Spyrou, A. Avgeropoulos, D. Gournis and H. Stamatis, *Micromachines*, 2022, **13**(11), 1954.
29 M. Chai, S. Razavi Bazaz, R. Daiyan, A. Razmjou, M. Ebrahimi Warkiani, R. Amal and V. Chen, *Chem. Eng. J.*, 2021, 426.
30 N. Büscher, C. Spille, J. K. Kracht, G. V. Sayoga, A. W. H. Dawood, M. I. Maiwald, D. Herzog, M. Schlüter and A. Liese, *Org. Process Res. Dev.*, 2020, **24**, 1621–1628.
31 A. Valotta, M. C. Maier, S. Soritz, M. Pauritsch, M. Koenig, D. Brouczek, M. Schwentenwein and H. Gruber-Woelfler, *J. Flow Chem.*, 2021, **11**, 675–689.
32 D. S. Wunschik, K. N. Ingenbosch, P. Suss, U. Liebelt, S. Quint, M. Dyllick-Brenzinger, R. Zuhse, U. Menyes, K. Hoffmann-Jacobsen, K. Opwis and J. S. Gutmann, *Enzyme Microb. Technol.*, 2020, **136**, 109512.
33 H. S. Kim, S.-G. Hong, J. Yang, Y. Ju, J. Ok, S.-J. Kwon, K.-M. Yeon, J. S. Dordick and J. Kim, *J. CO_2 Util.*, 2020, **38**, 291–298.
34 M. Pätzold, S. Siebenhaller, S. Kara, A. Liese, C. Syldatk and D. Holtmann, *Trends Biotechnol.*, 2019, **37**, 943–959.
35 S. R. Bazaz, A. A. Mehrizi, S. Ghorbani, S. Vasilescu, M. Asadnia and M. E. Warkiani, *RSC Adv.*, 2018, **8**, 33103–33120.
36 J. Hou, G. Qian and X. Zhou, *Chem. Eng. J.*, 2011, **167**, 475–482.
37 J. Yue, G. Chen, Q. Yuan, L. Luo and Y. Gonthier, *Chem. Eng. Sci.*, 2007, **62**, 2096–2108.
38 L. Pesci, M. Baydar, S. Glueck, K. Faber, A. Liese and S. Kara, *Org. Process Res. Dev.*, 2017, **21**, 85–93.
39 A. C. Daly, M. E. Prendergast, A. J. Hughes and J. A. Burdick, *Cell*, 2021, **184**, 18–32.
40 F. Qian, C. Zhu, J. M. Knipe, S. Ruelas, J. K. Stolaroff, J. R. DeOtte, E. B. Duoss, C. M. Spadaccini, C. A. Henard, M. T. Guarnieri and S. E. Baker, *Nano Lett.*, 2019, **19**, 5829–5835.
41 A. Saha, T. G. Johnston, R. T. Shafranek, C. J. Goodman, J. G. Zalatan, D. W. Storti, M. A. Ganter and A. Nelson, *ACS Appl. Mater. Interfaces*, 2018, **10**, 13373–13380.
42 F. He, Y. Ou, J. Liu, Q. Huang, B. Tang, F. Xin, J. Zhang, M. Jiang, S. Chen and Z. Yu, *Small*, 2022, **18**, 2104820.
43 Y. Liu, X. Xia, Z. Liu and M. Dong, *Small*, 2023, **19**, 2205949.
44 A. M. Duraj-Thatte, A. Manjula-Basavanna, J. Rutledge, J. Xia, S. Hassan, A. Sourlis, A. G. Rubio, A. Lesha, M. Zenkl, A. Kan, D. A. Weitz, Y. S. Zhang and N. S. Joshi, *Nat. Commun.*, 2021, 12.
45 Z. Cui, Y. Feng, F. Liu, L. Jiang and J. Yue, *ACS Macro Lett.*, 2022, **11**, 452–459.

46 K. Dubbin, Z. Dong, D. M. Park, J. Alvarado, J. Su, E. Wasson, C. Robertson, J. Jackson, A. Bose, M. L. Moya, Y. Jiao and W. F. Hynes, *Nano Lett.*, 2021, **21**, 1352–1359.
47 B. Lin and Y. Tao, *Microb. Cell Fact.*, 2017, **16**, 106.
48 M. R. Smith, E. Khera and F. Wen, *Ind. Eng. Chem. Res.*, 2015, **54**, 4021–4032.
49 J. Shen, S. Zhang, X. Fang and S. Salmon, *Gels*, 2022, **8**(8), 460.
50 J. Meyer, L. E. Meyer and S. Kara, *Eng. Life Sci.*, 2022, **22**, 165–177.
51 Y. Shao, Z. Liao, B. Gao and B. He, *ACS Omega*, 2022, **7**, 11530–11543.
52 M. Maier, C. P. Radtke, J. Hubbuch, C. M. Niemeyer and K. S. Rabe, *Angew. Chem., Int. Ed. Engl.*, 2018, **57**, 5539–5543.
53 B. Schmieg, J. Dobber, F. Kirschhofer, M. Pohl and M. Franzreb, *Front. Bioeng. Biotechnol.*, 2018, **6**, 211.
54 B. Schmieg, A. Schimek and M. Franzreb, *Eng. Life Sci.*, 2018, **18**, 659–667.
55 J. Liu, X. Shen, Z. Zheng, M. Li, X. Zhu, H. Cao and C. Cui, *Int. J. Biol. Macromol.*, 2020, **164**, 518–525.
56 A. Steier, B. Schmieg, Y. Irtel Von Brenndorff, M. Meier, H. Nirschl, M. Franzreb and J. Lahann, *Macromol. Biosci.*, 2020, **20**, 2000154.
57 X. Shen, M. Yang, C. Cui and H. Cao, *Colloids Surf., A*, 2019, **568**, 411–418.
58 Y. Shi, T. L. Xing, H. B. Zhang, R. X. Yin, S. M. Yang, J. Wei and W. J. Zhang, *Biomed. Mater.*, 2018, **13**, 035008.
59 A. K. Tamo, T. A. Tran, I. Doench, S. Jahangir, A. Lall, L. David, C. Peniche-Covas, A. Walther and A. Osorio-Madrazo, *Materials*, 2022, **15**, 6039.
60 F. Croci, J. Vilim, T. Adamopoulou, V. Tseliou, P. J. Schoenmakers, T. Knaus and F. G. Mutti, *Chembiochem*, 2022, **23**, e202200549.
61 M. Peng, E. Mittmann, L. Wenger, J. Hubbuch, M. K. M. Engqvist, C. M. Niemeyer and K. S. Rabe, *Chemistry*, 2019, **25**, 15998–16001.
62 C. K. Dixit, K. Kadimisetty and J. Rusling, *Trends Anal. Chem.*, 2018, **106**, 37–52.
63 W. Hou, A. Bubliauskas, P. J. Kitson, J.-P. Francoia, H. Powell-Davies, J. M. P. Gutierrez, P. Frei, J. S. Manzano and L. Cronin, *ACS Cent. Sci.*, 2021, **7**, 212–218.
64 S.-H. Jun, J. Yang, H. Jeon, H. S. Kim, S. P. Pack, E. Jin and J. Kim, *Environ. Sci. Technol.*, 2020, **54**, 1223–1231.
65 J. Pakkanen, D. Manfredi, P. Minetola and L. Iuliano, in *Sustainable Design and Manufacturing*, 2017, ch. 73, pp. 776–785.
66 M. B. Salehi and A. M. Moghadam, in *Sustainable Hydrogels*, ed. S. Thomas, B. Sharma, P. Jain and S. Shekhar, Elsevier, 2023, pp. 23–46.
67 P. Zhao, C. Rao, F. Gu, N. Sharmin and J. Fu, *J. Cleaner Prod.*, 2018, **197**, 1046–1055.
68 M. Dieterle and J. Ginter, *Procedia CIRP*, 2022, **105**, 13–18.
69 M. F. Cosate De Andrade, P. M. S. Souza, O. Cavalett and A. R. Morales, *J. Polym. Environ.*, 2016, **24**, 372–384.
70 B. Xu, Y. Chen, J. He, S. Cao, J. Liu, R. Xue, F. Xin, X. Qian, J. Zhou, W. Dong and M. Jiang, *Environ. Rev.*, 2021, **30**, 30–38.
71 R. Yang, G. Xu, B. Dong, H. Hou and Q. Wang, *Macromolecules*, 2022, **55**, 1726–1735.
72 J. Finnerty, S. Rowe, T. Howard, S. Connolly, C. Doran, D. M. Devine, N. M. Gately, V. Chyzna, A. Portela, G. S. N. Bezerra, P. McDonald and D. M. Colbert, *J. Compos. Sci.*, 2023, **7**, 141.
73 A. N. Mistry, B. Kachenchart, A. Wongthanaroj, A. Somwangthanaroj and E. Luepromchai, *Polym. Degrad. Stab.*, 2022, **202**, 110051.
74 J. Yu, P. D. Kim, Y. Jang, S.-K. Kim, J. Han and J. Min, *Biodegradation*, 2022, **33**, 477–487.
75 V. Hotař, M. Stará, V. Máková and B. N. Holubová, *Pure Appl. Chem.*, 2022, **94**, 169–179.
76 C. Liu, T. Oriekhov and M. Fokine, *Front. Mater.*, 2022, **9**, 978861.
77 E. Gal-Or, Y. Gershoni, G. Scotti, S. M. E. Nilsson, J. Saarinen, V. Jokinen, C. J. Strachan, G. Boije af Gennäs, J. Yli-Kauhaluoma and T. Kotiaho, *Anal. Methods*, 2019, **11**, 1802–1810.
78 R. A. Rocha, L. Esquirol, V. Rolland, P. Hands, R. E. Speight and C. Scott, *Enzyme Microb. Technol.*, 2023, **169**, 110268.
79 S. Gallus, E. Mittmann, A. J. Weber, M. Peng, C. M. Niemeyer and K. S. Rabe, *ChemCatChem*, 2023, 15.
80 Q. Chen, Y. Wang and G. Luo, *ChemSusChem*, 2023, **16**, e202201654.
81 Y. Pinyakit, P. Romphophak, P. Painmanakul and V. P. Hoven, *Biomacromolecules*, 2023, **24**, 3138–3148.
82 S. C. Cosgrove, G. J. Miller, A. Bornadel and B. Dominguez, *ACS Sustainable Chem. Eng.*, 2023, **11**, 8556–8561.
83 T. Burgahn, P. Pietrek, R. Dittmeyer, K. S. Rabe and C. M. Niemeyer, *ChemCatChem*, 2020, **12**, 2452–2460.
84 P. Bitterwolf, A. E. Zoheir, J. Hertel, S. Kröll, K. S. Rabe and C. M. Niemeyer, *Chem.–Eur. J.*, 2022, **28**, e202202157.
85 N. Adebar, A. Nastke, J. Löwe and H. Gröger, *Angew. Chem., Int. Ed.*, 2021, **60**, 15863–15869.
86 B. Poznansky, L. A. Thompson, S. A. Warren, H. A. Reeve and K. A. Vincent, *Org. Process Res. Dev.*, 2020, **24**, 2281–2287.
87 A. Kazan, X. Hu, A. Stahl, H. Frerichs, I. Smirnova and O. Yesil-Celiktas, *J. Chem. Technol. Biotechnol.*, 2021, **96**, 3349–3357.
88 L.-H. Du, M. Xue, M.-J. Yang, Y. Pan, L.-Y. Zheng, Z.-M. Ou and X.-P. Luo, *Catalysts*, 2020, **10**, 1419.
89 L. A. Thompson, J. S. Rowbotham, J. H. Nicholson, M. A. Ramirez, C. Zor, H. A. Reeve, N. Grobert and K. A. Vincent, *ChemCatChem*, 2020, **12**, 3913–3918.
90 E. Gkantzou, K. Govatsi, A. V. Chatzikonstantinou, S. N. Yannopoulos and H. Stamatis, *ACS Sustainable Chem. Eng.*, 2021, **9**, 7658–7667.
91 C. Wang, X. P. Tan, S. B. Tor and C. S. Lim, *Addit. Manuf.*, 2020, **36**, 101538.
92 M. Piovarči, M. Foshey, J. Xu, T. Erps, V. Babaei, P. Didyk, S. Rusinkiewicz, W. Matusik and B. Bickel, *ACM Trans. Graph.*, 2022, **41**, 1–10.